Journal of
Nanoscience and Nanotechnology
Vol. 9, 1–5, 2009

Fabrication of Nano-Structured Hemispheres and Pillars Using Laterally Migrating Polymer Templates

Hye Jin Nam[1], Gi-Ra Yi[2], Seong-Hun Jeong[3], Jin-Hyo Boo[3], and Duk-Young Jung[1,*]

[1] *Department of Chemistry-BK21, Institute of Basic Sciences, SKKU Advanced Institute of Nano Technology (SAINT), Sungkyunkwan University, Suwon 440-746, South Korea*
[2] *Institute of Nano-Biosystem, Korea Basic Science Institute (KBSI), 5-Ka, Anam-Dong, Sungbuk-Gu, Seoul 136-701, South Korea*
[3] *Department of Chemistry-BK21, Institute of Basic Sciences, Sungkyunkwan University, Suwon 440-746, South Korea*

We report herein a reliable method of fabricating 2D periodic gold nanopillars with well-defined anisotropic shapes by the combinational actions of colloidal crystals and gold evaporation. The deposition of gold on a polymer template produced dual functional Janus-like nanopillars up to 633 nm in height as well as hemispherical shells with 120 nm. The thermal-induced active migration of the nanopillars from the pristine position in the lateral direction occurred at the colloidal defects while some cavity space was formed inside the gold pillars. The nano-structured gold pillars exhibited a strong surface plasmon resonance at 598 nm, as compared to that of the solid gold nanospheres at 520 nm, and a noticeable red shift to 640 nm was induced by the removal of the polymer template.

Keywords: Gold Nanopillar, Hemisphere, Colloidal Crystal, Nanocomposite, Migration.

Surface patterning using colloidal spheres has recently become an important issue, because of their potential applications in photoelectronics and biological sensor materials.[1–4] Ordered colloidal crystals of polymers have been used as a template for multidimensional periodic nanoporous materials or lithographic etching, as well as a mask for triangular patterns to produce patterned nanostructures.[5–9] Nanoporous structures show unique surface plasmon resonance (SPR) depending on the shell thickness and template medium, in comparison with their solid counterparts.[10] The red shifts of the SPR bands caused by the removal of the template have recently been reported for colloidal-templated metallic nanostructures.[11] When the colloidal templates are removed by solution etching, the topographical loss of the nanoporous structures could be occurred,[12, 13] making it difficult to control their optical properties. Thus, the non-solution removal of the template using techniques such as pyrolysis is preferable to prevent the loss of the nanostructures of the prepared materials.

The deposition of gold on a PS colloidal template produces ordered dual functional Janus particles with an anisotropic shape, consisting of two different hemispheres of PS and gold. There are some instances for fabricating biphasic Janus particles by surface modification of microspheres using solution deposition technique.[14–16] However, these techniques have limitations in varying shapes and aspect ratios of the prepared particles. On the other hand, thermal evaporation enables us to produce such hybrid and unique structures with various aspect ratios. These dual functional Janus structures are highly useful for controlling the optical and wetting properties, due to their unique ability to allow the chemical modification of the gold hemisphere to be achieved using functional derivatives.[17] The deposition of gold provides a variable surface charge on the gold hemisphere so as to form amphiphilic nanostructures, which are applicable for photonic and electronic devices such as biosensors or electronic paper.

The deposition of gold leads to the 2D rearrangement of the gold-on-PS particles and the removal of the template by thermal treatment enhances the rearrangement. Since the resulting nanostructure greatly depends on the characteristics of the template, tailoring the topographical movement of the colloidal templates is a prerequisite condition for obtaining high quality engineered materials. However, the unpredictable defects in the colloidal crystal hamper the production of the desired surface. The 2D defects modify the physical properties of the deposited materials such as density, electrical conductivity as well as the reorganization of the colloidal template with respect to the surface free energy of the interface. In addition to the defects by

*Author to whom correspondence should be addressed.

COMMUNICATION

thermal treatment, the 2D defects change by melting or applied external force,[18, 19] and produce surface voids with nanometer to micrometer sizes, capable of generating new functional nano-structured materials. Although the melting behavior of colloidal crystals has been actively studied by theoretical simulation methods, systematic investigations on the thermal motion of colloids have rarely been reported.[20–22]

In this paper, we report a versatile synthetic strategy for fabricating Janus-like nano-structured gold pillars with controllable aspect ratios by exploiting ordered 2D polymer crystals and gold deposition. The modification of the structure of the nanopillars was attempted by varying the gold layer thickness and thermal treatment time, and the changes in the thermodynamic and optical behaviors caused by the surface defects of the nanopillars were investigated. We suggest several important experimental parameters to produce pre-designed gold nanopillars and bring about thermally induced dynamic motions, which could quantify the spatial extent of the migrations during the 2D melting.

The preparation consists of two processes: fabrication of two-dimensional colloidal crystal and gold deposition. The glass slides were cleaned with piranha solution, 3:1 H_2SO_4/H_2O_2, to remove the residual organic impurities, sonicated for 30 minutes, and then washed with deionized water with a resistivity of 18 $M\Omega \cdot cm$ and isopropyl alcohol. The substrates were dried in a nitrogen stream and retreated with an oxygen plasma (Harrick, 30 W). A two-dimensional colloidal monolayer was prepared by the spin-casting of the 10 wt% aqueous colloidal solution (Microparticles GmbH, Germany) of polystyrene microspheres with a diameter of 345 nm at 3000 rpm for 30 seconds. The PS 2D crystal was then treated at 70 °C for 1 hour to reliably attach the PS microspheres onto glass surface by slight melting. Details of the experimental procedures and the morphology controlled 2D crystals can be found in our previous report.[23] Vacuum thermal evaporation using gold wire (99.99%, Nilaco, Japan) is used to deposit the gold layer onto the PS crystal template. The 30 nm to 300 nm thick gold layers were deposited at a constant evaporation rate of ~2 Å/s onto the PS arrays, where the deposition times were controlled to 20, 40, 80 and 120 seconds, respectively. The substrates were placed on a sample holder at a distance of 40 mm from the tungsten boat and the evaporation system was typically operated at a pressure of $<10^{-2}$ Torr. After the evaporation, the gold-coated PS crystals formed Au/PS composite nanopillars and finally gold nanopillars were obtained after removal of PS template by annealing at 300 °C for 30 minutes or 1 hour.

Figure 1 shows the schematic illustration and SEM (JSM-7000F, JEOL) images for fabrication and thermal treatment of gold nanopillars. The gold layer depositions (Figs. 1(a–d)) and thermal treatments (Figs. 1(e–h)) gave

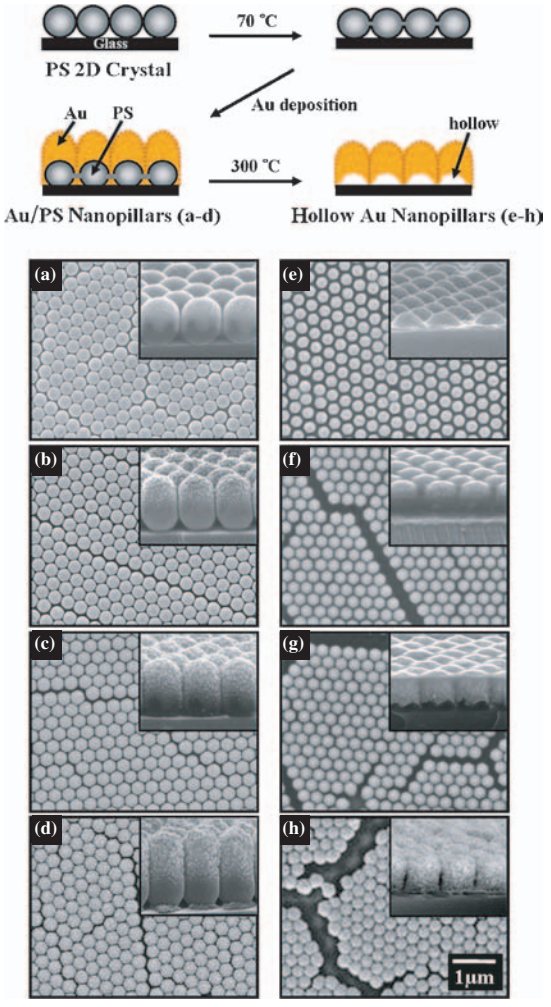

Fig. 1. Schematic illustration (top) and SEM images (bottom) of gold nanopillars before (a–d) and after (e–h) pyrolysis at 300 °C for 30 minutes for 20 s (a, e), 40 s (b, f), 80 s (c, g) and 120 s deposition time (d, h). The insets show higher-magnification SEM images for plane-view (left) and side-view (right), respectively.

nanopillars with spherical tops and nano-sized cavities beneath the gold layer. The thermal treatment led to the structural transformation of the Au/PS layer from spherical to hemispherical, with the height of the pillars being remarkably decreased from 360 nm to 180 nm, indicating the absence of a gold layer underneath the equator of the PS microspheres. Despite the deposition of a thin layer of gold, the prepared hemispherical nanostructures were sufficiently robust for them not to collapse up to 300 °C. Upon increasing the thickness of the gold layer, the population of the clusterized gold grains gradually increased, producing rough and textured morphologies.

The pyrolysis of the PS template produced submicrometer-sized voids and a remarkable change in the 2D structure of the gold pillars as shown in Figure 2. The variations of the center-to-center distances between the gold pillars were correlated with the configurational changes of the voids for the three different nanostructures,

COMMUNICATION

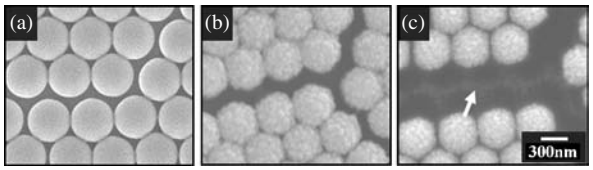

Fig. 2. SEM images demonstrating the variation of center-to-center distance at defect for PS 2D crystal (a), 120 s-coated Au/PS composite nanopillar (b) and hollow gold nanopillar (c). The white arrow shows the gold trace layer deposited on the void area of PS 2D crystal.

viz. the PS 2D crystals (Fig. 2(a)), Au/PS nanopillars (Fig. 2(b)) and hollow gold nanopillars (Fig. 2(c)). The center-to-center distance of the PS spheres was increased from 325 nm to 375 nm by the reduction of the hydrodynamic diameter during the crystallization of PS[24] and was further enlarged to 417 nm by the deposition of gold on the PS monolayer, which simultaneously induced the deformation of the nanopillars to hexagonal shapes due to the close-contacts. The larger thermal expansion coefficient of PS than those of glass and gold caused the enhancement of the close-contacts between the nanopillars.[25–27] Upon increasing the deposition time of gold, the void distances increased from 254 nm to 639 nm. Traces of the gold layer deposited on the void spaces were simultaneously observed in the defect regions, and were clearly seen in the thicker gold films, implying the larger migration of the nanopillars in the lateral direction by 2D melting in the case of the thicker gold films.[28] Prolonging the thermal treatment resulted in a considerable increase in the void area ratio, with thermal treatment for 1 hour leading to a void area ratio 8% larger than that observed after 30 min.

The packing mismatch at the defects drives the melting process to minimize the interfacial free energy caused by the surface tension during the thermal treatment, resulting in the structural variation of the nanopillars. Thus, the PS colloidal crystal has the potential to develop the designed rearrangement of nano-structured pillars. In addition to the thermal-induced migration, other external forces could be involved in the modification of the topographic defects, for instance, the mechanical vibration demonstrated by Wu et al.[19] Herein, we investigated the gravitational movement of the Au/PS composite pillars in the vertical orientation by thermal treatment to rearrange the void areas. Gravitational force gave rise to the longitudinal sliding movement of the nanopillars from the top to the bottom region, in which case the area coverage ratio of the particle-occupied region to the total film area increased from 81.7% to 88.3%, producing one-dimensional void gradient nanostructures.

The as-grown Au/PS pillars had diameters of around 324 nm irrespective of the thickness of the gold layer, while the height of the pillars increased from 360 nm to 633 nm at an average growth rate of about 5 nm/s, as shown in Figures 3(a and b). The thermal treatment of the nanocomposite pillars caused a decrease in the diameters

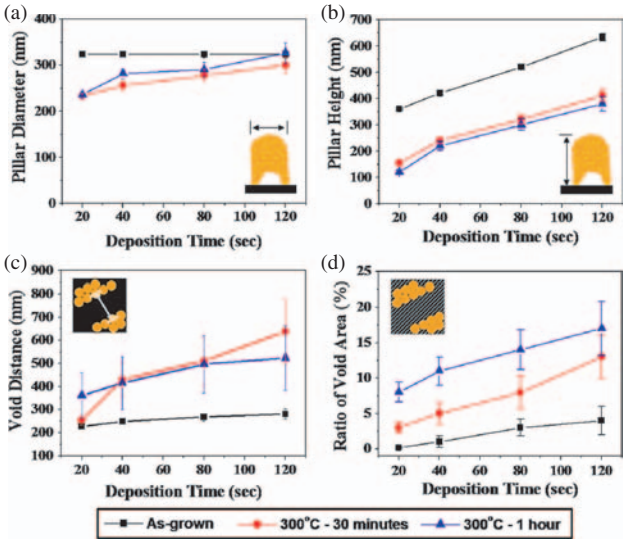

Fig. 3. Pillar diameters (a), pillar heights (b), average distance of gaps (c) and ratio of void areas to total film area (d) as a function of deposition time.

of the pillars, with the diameters of the annealed pillars being 233 nm for the thin Au/PS and 300 nm for the thick sample, indicating the larger shrinkage in the case of the thinner layered gold pillars, due to the proportionally greater collapse. The pyrolysis of PS also induced a noticeable decrease in their height of about 50% for the largest variation. As the thickness of the gold layer increased, the void distances increased from 227 to 281 nm and the thermal treatment allowed this value to increase up to 639 nm, as presented in Figure 3(c). The large variation of the error bars in the void distances is ascribed to the difference in the void widths between the small dislocations and the large grain boundaries. The void area ratios showed linear dependence on the thickness of the layer and thermal treatment time, as shown in Figure 3(d). The quasi-constant variation of the void ratios indicates the possible tuning of the void area ratios to the target values.

Based on the Lindemann parameter, L, which estimates the mean-square displacement (MSD) of particles at the melting transition, we examined the thermal-induced fluctuations for the three prepared nanostructures at the grain boundaries, viz. the Au/PS nanopillars in the as-grown state and heated for 30 min and 1 h, respectively, using the relation for a 2D colloidal system.[28] The linear dependences of the MSD and L on the thermal treatment time of the gold layer were observed, with the L values for the three samples being 0.162, 1.958 and 0.503, respectively. Usually, the L values in a colloidal crystal are known to be ~0.12 for melting and ~0.18 for premelting,[22] indicating the notable L values obtained in this study, thanks to the large particle movement at the grain boundaries during the thermal treatment.

The Au/PS nanocomposites present a novel anisotropic "Janus"-like structure consisting of PS and gold. From

COMMUNICATION

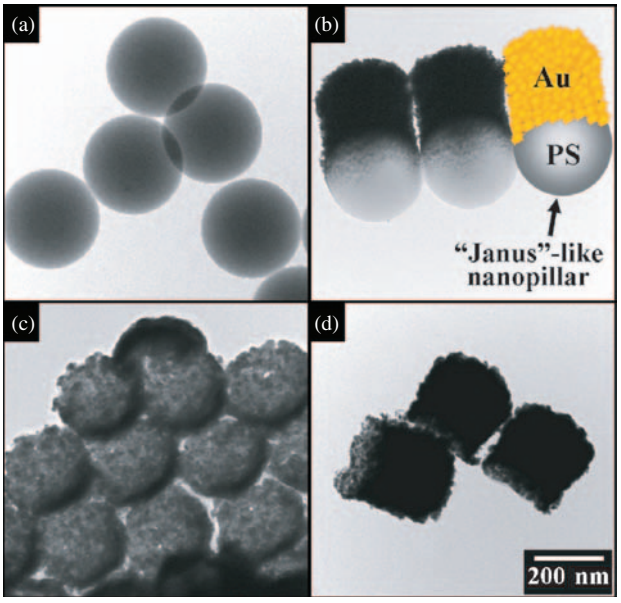

Fig. 4. TEM images of the nanostructured pillars depending on gold thickness; (a) 325 nm PS microspheres, (b) 120 s-coated Au/PS composite pillars, (c) 40 s-coated gold nanopillars and (d) 120 s-coated gold nanopillars.

the TEM (FE-TEM, JEM 2100F, JEOL) images shown in Figure 4, we could confirm that the hemisphere of PS (Fig. 4(a)) in the nanocomposite structure (Fig. 4(b)) is covered with aggregated gold nanoparticles and that the deposition of a thin layer of gold produces a hollow architecture with nanopores (Figs. 4(c and d)). Figure 5 shows the SEM images of the gold nanostructures with cavity before (Fig. 5(a)) and after focused ion beam (FIB, FEI Qunata 200)-etching (Figs. 5(b and c)). FIB milling and transfer onto carbon tape (Fig. 5(d)) allowed the Janus shapes and hollow interiors of the gold nanostructures to

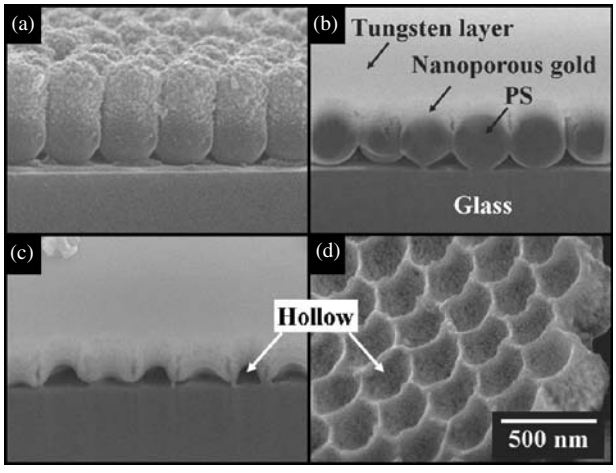

Fig. 5. SEM data for (a) as-deposited 120 s Au/PS nanopillars, (b) FIB-etched Au/PS nanopillars, (c) FIB-etched gold nanopillars with cavity and (d) the back-side image obtained by peel-off, showing hollow cavities beneath gold nanopillars.

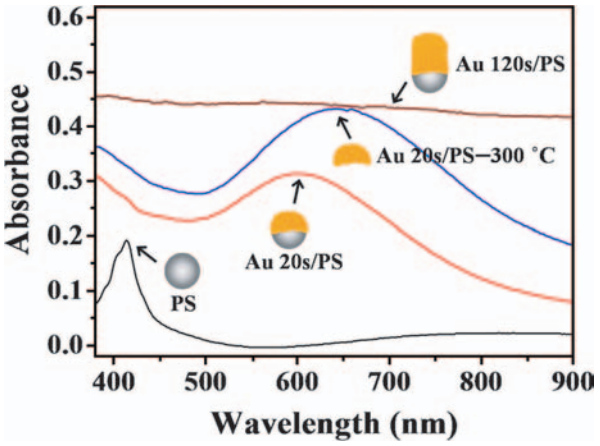

Fig. 6. UV-Vis absorption spectra of gold nanopillars showing characteristic red-shift of surface plasmon resonance bands depending on gold thickness.

be clearly observed. First, a tungsten layer with dimensions of 10 μm (width) $\times$ 2 μm (height) was deposited onto the 120 s-coated Au/PS nanopillars and hollow gold nanopillars formed by annealing at 300 °C for 30 min to prevent them from collapsing due to the ion beam, followed by ion milling by Ga ions. The Janus-like Au/PS particles present sufficiently robust gold-PS adhesion for them to maintain their as-prepared shape after their dispersion in solution under ultrasonic treatment, indicating their potential application in the formation of new 2D nanostructured materials at air–water interfaces.

The UV/vis (Hitachi UV-4100) data of the Au/PS pillars exhibited characteristic SPR properties depending on the thickness of the gold layer, as shown in Figure 6. The band of the PS crystals was observed at around 410 nm. The SPR band of the thin-layered gold pillars was observed at 598 nm, indicating that it was red-shifted compared to those of citrate-capped gold nanoparticles and nano-sized gold spheres,[29, 30] presumably due to the aggregation of the nano-sized gold grains. The broad bands are ascribed to the dipole–dipole interaction between the aggregated particles.[31] The SPR band and red-shift disappeared for the gold/PS nanopillars greater than 500 nm in height. The 180 nm gold hemispheres underwent a change of their refractive index upon the removal of the PS template[32] and a remarkable red-shift of the SPR band to 643 nm was observed, along with its substantial broadening due to the increase of the aggregated gold nanoparticles based on Mie scattering theory.[33] The present method provides a facile tool to tailor the optical properties of metal nanostructures depending on the applied polymers and metals.

In summary, we fabricated 2D systems consisting of Janus-like nanopillars to demonstrate the design of novel gold nanostructures. The thermal expansion of the void areas provided numerical data on the 2D migration of the gold pillars and suggested that the maximum displacement occurred at the grain boundaries. These results confirm

COMMUNICATION

the feasibility of conducting further experiments to change the colloidal crystal density and particle arrangement, for instance, the sliding of particles by mechanical vibration and gravitational force. The optimized gold hemispheres showed a remarkable shift of the SPR bands up to 120 nm, indicating the potential capability to prepare promising functional materials with pre-tuned optical and photonic properties. We expect that the present synthetic strategy would enable the surface architecture of nano-structured films, including colloidal crystals, to be tailored, while allowing for the adjustment of the optical properties.

Acknowledgments: This work was supported by the Brain Korea (BK)-21 program, the Korea Research Foundation Grant funded by Korean government (MOEHRD) (KRF-2005-005-J11902) and the National Research Laboratory Program of Korea Science and Engineering Foundation (Program No. ROA-2007-000-10020-0).

References and Notes

1. J. Wang, Y. Cao, Y. Feng, F. Yin, and J. Gao, *Adv. Mater.* 19, 3865 (**2007**).
2. M. E. Abdelsalam, S. Mahajan, P. N. Bartlett, J. J. Baumberg, and A. E. Russell, *J. Am. Chem. Soc.* 129, 7399 (**2007**).
3. S. Sun, C. B. Murray, D. Weller, L. Folks, and A. Moser, *Science* 287, 1989 (**2000**).
4. J. P. Walker and S. A. Asher, *Anal. Chem.* 77, 1596 (**2005**).
5. P. N. Bartlett, J. J. Baumberg, P. R. Birkin, M. A. Ghanem, and M. C. Netti, *Chem. Mater.* 14, 2199 (**2002**).
6. A. Stein, F. Li, and N. R. Denny, *Chem. Mater.* 20, 649 (**2008**).
7. I. D. Kim, A. Rothschild, T. Hyodo, and H. L. Tuller, *Nano Lett.* 6, 193 (**2006**).
8. D.-G. Choi, H. K. Yu, S. G. Jang, and S.-M. Yang, *J. Am. Chem. Soc.* 126, 7019 (**2004**).
9. C. L. Haynes, A. D. McFarland, M. T. Smith, J. C. Hulteen, and R. P. Van Duyne, *J. Phys. Chem. B* 106, 1898 (**2002**).
10. H. P. Liang, L. J. Wan, C. L. Bai, and L. Jiang, *J. Phys. Chem. B* 109, 7795 (**2005**).
11. W. Shi, Y. Sahoo, M. T. Swihart, and P. N. Prasad, *Langmuir* 21, 1610 (**2005**).
12. J. C. Love, B. D. Gates, D. B. Wolfe, K. E. Paul, and G. M. Whitesides, *Nano Lett.* 2, 891 (**2002**).
13. A. Imhof, *Langmuir* 17, 3579 (**2001**).
14. K. Fujimoto, K. Nakahama, M. Shidara, and H. Kawaguchi, *Langmuir* 15, 4630 (**1999**).
15. V. N. Paunov and O. J. Cayre, *Adv. Mater.* 16, 788 (**2004**).
16. A. Perro, S. Reculusa, S. Ravaine, E. Bourgeat-Lamic, and E. Duguet, *J. Mater. Chem.* 15, 3745 (**2005**).
17. D. Suzuki and H. Kawaguchi, *Colloid Polym. Sci.* 284, 1471 (**2006**)
18. P. N. Pusey, *Science* 309, 1198 (**2005**).
19. Q. H. Wei and X. L. Wu, *Phys. Rev. E* 70, 020401 (**2004**).
20. C. Reichhardt and C. J. O. Reichhardt, *Phys. Rev. Lett.* 92, 108301 (**2004**).
21. S. Xiao and W. Hu, *J. Chem. Phys.* 125, 014503 (**2006**).
22. A. M. Alsayed, M. F. Islam, J. Zhang, P. J. Collings, and A. G. Yodh, *Science* 309, 1207 (**2005**).
23. H. J. Nam, D.-Y. Jung, G.-R. Yi, and H. Choi, *Langmuir* 22, 7358 (**2006**).
24. Y. Kusaka and Y. Adachi, *Colloids Surf. A: Physicochem. Eng. Aspects* 306, 166 (**2007**).
25. J. F. Rudd, Polymer Handbook, 3rd edn., edited by J. Brandrup and E. H. Immergut, Wiley, New York (**1989**), p. V/81.
26. M. Stjernström and J. Roeraade, *J. Micromech. Microeng.* 8, 33 (**1998**).
27. P. J. de Pablo, J. Colchero, J. Gómez-Herrero, P. A. Serena, and A. M. Baró, *Nanotechnology* 12, 113 (**2001**).
28. J. Bongers and H. Versmold, *J. Chem. Phys.* 104, 1519 (**1996**).
29. W. Shi, Y. Sahoo, M. T. Swihart, and P. N. Prasad, *Langmuir* 21, 1610 (**2005**).
30. T. Ung, L. M. Liz-Marzán, and P. Mulvaney, *J. Phys. Chem. B* 105, 3441 (**2001**).
31. K. E. Peceros, X. Xu, S. R. Bulcock, and M. B. Cortie, *J. Phys. Chem. B* 109, 21516 (**2005**).
32. Z. Liang, A. Susha, and F. Caruso, *Chem. Mater.* 15, 3176 (**2003**).
33. S. Vial, I. Pastoriza-Santos, J. Pérez-Juste, and L. M. Liz-Marzán, *Langmuir* 23, 4606 (**2007**).

Received: 13 October 2008. Accepted: 13 November 2008.

COMMUNICATION